PHYSICAL REVIEW D VOLUME 39, NUMBER 1 1 JANUARY 1989

Measuring the parton content of the photon at the DESY *ep* collider HERA

Manuel Drees
Physics Department, University of Wisconsin, Madison, Wisconsin 53706

R. M. Godbole*
Institut für Physik, Universität Dortmund, 4600 Dortmund 50, West Germany
(Received 13 May 1988; revised manuscript received 31 August 1988)

We discuss the possibility to measure the parton, and especially gluon, content of the photon at the forthcoming DESY *ep* collider HERA. We first reemphasize that the production of two jets with high transverse momentum p_T is dominated by events where the photon is resolved into quarks and gluons for $p_T \lesssim 40$ GeV. We then show that these "resolved" contributions, and in particular those that are initiated by a gluon from the photon, are especially important at large jet rapidities. Rapidity distributions also allow us to isolate the direct photon-gluon fusion contributions to $b\bar{b}$ production. This makes it possible to use this process to determine the gluon content of the proton. However, a direct measurement of the gluon content of the photon will only be possible if the spectator jet from the photon can be detected. We find that this jet typically has an energy of 10–12 GeV and estimate its opening angle to be around 15°, which should allow for its detection.

I. INTRODUCTION

The hadronic structure of the photon has, for some time, been thought to be an ideal testing ground for perturbative QCD. This optimism was triggered by Witten's discovery[1] that in the limit of very-high-momentum transfer Q^2 the quark and gluon distributions inside the photon are completely calculable; this calculation has subsequently been extended to two-loop order by Bardeen and Buras.[2] However, these "asymptotic" solutions of the evolution equations[3] for $\mathbf{q}^\gamma \equiv (q_i^\gamma, G^\gamma)$ lead to unphysical $x \to 0$ divergences in F_2^γ; the degree of the pole increases in higher order of perturbation theory.[2,4] On the other hand, if one introduces[5] input distributions $q_i^\gamma(Q_0^2)$, $G^\gamma(Q_0^2)$ at some scale Q_0^2 such that $F_2^\gamma(x, Q_0^2)$ is finite for all x, the solution of the evolution equations automatically leads to a well-behaved F_2^γ at all values of Q^2.

Of course, the introduction of the unknown functions $q_i^\gamma(Q_0^2)$ and $G^\gamma(Q_0^2)$ means that only the Q^2 evolution can be predicted by QCD. Antoniadis and Grunberg[6] therefore suggested to keep only those parts of $\mathbf{q}^\gamma(Q_0^2)$ that are necessary to remove the $x \to 0$ divergences in F_2^γ. In second order this amounts to the introduction of two unknown parameters instead of three unknown functions of the aforementioned approach; moreover, the value of these parameters only affects the region of small Bjorken x. However, it is *a priori* not clear that the unknown purely hadronic component of $\mathbf{q}^\gamma$ is only relevant for small values of x. Note that the Q^2 dependence of this part of $\mathbf{q}^\gamma$ is exactly like that of the parton distribution in any hadron, i.e., rather weak; it takes therefore many decades in Q^2/Q_0^2 to "shrink" $\mathbf{q}^\gamma(Q_0^2)$ to small x values. Even though the "asymptotic" or "pointlike" part of $\mathbf{q}^\gamma$ increases $\sim \ln Q^2$ this means that $\mathbf{q}^\gamma(Q_0^2)$ affects the prediction for F_2^γ even for medium and large values of x for all values of Q^2 accessible at the DESY e^+e^- storage ring PETRA, i.e., $Q^2 \lesssim 100$ GeV^2, even if one chooses[7] Q_0^2 as small as 1 GeV^2.

Theoretically, the problem of whether or not the "asymptotic " prediction of $\mathbf{q}^\gamma$ is reliable is still not settled.[8] This question is quite important since a fit of F_2^γ as predicted in Ref. 6 to existing data[9] yields a value of the QCD scale parameter $\Lambda_{\overline{\rm MS}}$ with a very small *statistical* error.[10] ($\overline{\rm MS}$ denotes the modified minimal-subtraction scheme.) However, the same data are compatible[11] with bigger values of $\Lambda_{\overline{\rm MS}}$ if one allows for a nonvanishing $\mathbf{q}^\gamma(Q_0^2)$, and can even be explained[10] in a naive quark-parton model (QPM) with "reasonable" constituent masses for u,d,s quarks. Obviously, additional experimental information is necessary.

Unfortunately, deep-inelastic scattering experiments at e^+e^- colliders will probably not be able to provide this information, for the following two reasons.

(i) The cross section for the scattering of a virtual probing photon with squared momentum $-Q^2$ off an on-shell photon is very small, $O(\alpha_{\rm em}^4(s/Q^4)\ln(s/m_e^2))$; it will therefore be hard to accumulate enough events.

(ii) The electromagnetic structure function F_2^γ measured in this type of experiment depends only very weakly on G^γ. A real test of QCD as opposed to the QPM will therefore be hard.

Another possible source of information on the hadronic structure of the photon is the two-photon production of two high-p_T jets at forthcoming e^+e^- colliders. Since now both photons are almost on shell, the corresponding cross section is somewhat bigger than in the deep-inelastic case, $O(\alpha_{\rm em}^4 p_T^{-2}(\ln s/m_e^2)^2)$. However, since both the photon distribution inside the electron and the gluon distribution inside the photon are rather soft, the next generation of e^+e^- colliders [SLAC Linear Collider (SLC) and CERN LEP] will probably not be able to measure the gluon content of the photon. In contrast,

photon-hadron scattering offers large cross sections and is sensitive to G^γ.

It has been realized some time ago by Owens[12] that in principle predictions for the production of inclusive or semi-inclusive final states in hard γp scattering depend on $\mathbf{q}^\gamma$. However, since the energy of existing photon beams is rather small [$\sqrt{s}(\gamma p) \lesssim 15$ GeV] the contributions proportional to $\mathbf{q}^\gamma$ are rather small[12–14] in the kinematic regions where perturbative QCD is applicable, i.e., $p_T \gtrsim 2-3$ GeV.

As we have shown in a recent Letter,[15] the situation is very different at the forthcoming DESY *ep* collider HERA where $\sqrt{s}(\gamma p)$ can be as large as 300 GeV. Here contributions proportional to $\mathbf{q}^\gamma$, Fig. 1(a), *dominate* the two-jet cross section up to jet transverse momenta $p_T \lesssim 40$ GeV; for $p_T \lesssim 10$ GeV these contributions where the photon is resolved into quarks and gluons ("resolved" contribution) are at least 4 times bigger than those where the photon couples directly to the partons in the photon ["direct" contributions, see Fig. 1(b)]. This clearly shows that the resolved contributions should *not* be treated as a rather small correction to the direct ones, on a par with higher-order QCD corrections. Note that the "asymptotic" part of $\mathbf{q}^\gamma$ is proportional to $\alpha_{\rm em}/\alpha_s$; direct and resolved contributions are therefore of the *same* order in $\alpha_{\rm em}$ and α_s. In this paper we investigate the possibility to measure $\mathbf{q}^\gamma$, and especially G^γ, via the resolved contribution to the production of two jets or a heavy-quark–antiquark pair.

The remainder of this paper is organized as follows. In Sec. II we reanalyze the transverse-momentum distribution $d\sigma(jj)/dp_T$ of two-jet events; we address technical points such as the reliability of the Weizsäcker-Williams approximation[16] (WWA) and the question to what extent the parton distributions in the *proton* have to be known before $\mathbf{q}^\gamma$ can be measured. In Sec. III we investigate in some detail the triple-differential two-jet cross section $d^3\sigma(jj)/dp_T dy_1 dy_2$ where $y_{1,2}$ are the jet rapidities. We find that direct and resolved contributions populate very different regions in (y_1,y_2) space; even contributions proportional to q_i^γ might be separable from those $\sim G^\gamma$ by virtue of their different rapidity distributions. In Sec. IV we use similar methods to study $b\bar{b}$ production. Even though the total cross section here is dominated[15] by direct photon-gluon fusion, a determination of G^γ might be possible by focusing onto the region of large rapidities, $y \gtrsim 3$, even in the absence of any other criterion to separate direct from resolved contributions. In Sec. V we assess the question whether the existence of a second spectator jet in the resolved events [see Fig. 1(a)] might allow us to tag directly on this class of events. We find that the average jet energy in the laboratory frame is rather low, $\langle E \rangle \simeq 10-12$ GeV, which presumably indicates a rather broad jet, the existence of which should not be too hard to verify. Finally, in Sec. VI we summarize our findings and draw some conclusions.

II. THE TRANSVERSE-MOMENTUM DISTRIBUTION OF TWO-JET EVENTS

The general expression for the *ep* photoproduction cross section for two high-p_T jets is, in the Weizsäcker-Williams approximation[16] (WWA),

$$\frac{d\sigma(jj)}{dp_T} = 2p_T \int_{4p_T^2/s}^1 dz\, f_{\gamma|e}(\bar{E},z) \int_{4p_T^2/\bar{s}}^1 dx_p \int_{4p_T^2/x_p\bar{s}}^1 dx_\gamma V_p(x_p,Q^2) V_\gamma(x_\gamma,Q^2) \frac{d\hat{\sigma}}{dp_T^2}(\hat{s},\hat{t},\hat{u}) \,. \tag{2.1}$$

Here, $s=(314\ \text{GeV})^2$ is the squared center-of-mass-system (c.m.s.) energy of the *ep* system, $\bar{s} \equiv zs$ is the squared c.m.s. energy of the γp system, and $\hat{s} \equiv x_p x_\gamma \bar{s}$ is the corresponding quantity in the parton-parton system (where the photon is counted as a parton in the case of the direct contributions). The functions V_p and V_γ are the parton densities inside the proton and photon, respectively, with $V_\gamma(x_\gamma,Q^2)=\delta(1-x_\gamma)$ for the direct contributions. The parton-parton scattering cross sections $\hat{\sigma}$ can, e.g., be found in Ref. 17 for the resolved contributions and Ref. 13 for the direct ones where for processes with two nonidentical final-state partons the $\hat{t} \leftrightarrow \hat{u}$ exchanged contribution has to be added. The Mandelstam variable $\hat{t}$ is given by

$$\hat{t} = \frac{\hat{s}}{2}\left[\frac{2m^2}{\hat{s}} - 1 + \left[1 - \frac{4m^2+4p_T^2}{\hat{s}}\right]^{1/2}\right], \tag{2.2}$$

where for further use we have allowed for a nonvanishing mass m of both final-state partons; in Secs. III and IV we will only consider the case $m=0$.

The function $f_{\gamma|e}$ describes the photon flux that originates from the electron beam. In leading-log approximation it is given by[16]

$$f_{\gamma|e}(\bar{E},z) = \frac{\alpha_{\rm em}}{2\pi} \frac{1+(1-z)^2}{z} \ln\frac{\bar{E}^2}{m_e^2} \,. \tag{2.3}$$

The question of what one should use for $\bar{E}^2$ is similar in nature to the problem of choosing the scale Q^2 in $\alpha_s(Q^2)$ and the parton densities in Eq. (2.1). However, in the former case we can directly test the quality of the WWA for different choices of $f_{\gamma|e}$ or $\bar{E}^2$ by considering only direct contributions where $d\sigma(jj)/dp_T$ can be computed without using the WWA. We focus here on the production of a massless quark-antiquark pair via photon-gluon fusion; the cross section is given by[18]

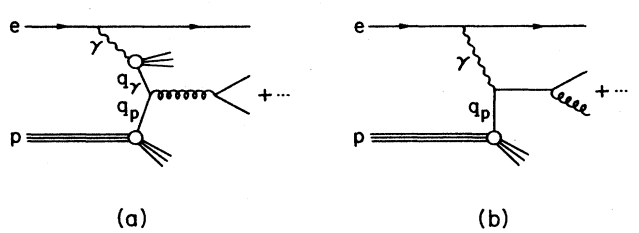

(a) (b)

FIG. 1. Typical Feynman diagrams for (a) resolved and (b) direct contributions to two-jet production at HERA.

$$\frac{d\sigma}{dp_T}=2p_T\int_{4p_T^2/s}^{1}dy\int_{m_e^2y/s(1-y)}^{1-4p_T^2/s\cdot y}dx\int_{x(1+4p_T^2/Q^2)}^{1}dz\frac{\alpha_{\rm em}^2\alpha_s(\hat{s})e_q^2G^p(z,\hat{s})}{\hat{s}Q^2xy(1-4p_T^2/\hat{s})^{1/2}}$$
$$\times\left\{\left[\frac{xy^2}{z}+\frac{2x(1-y)}{z}\right]\left[\frac{\hat{s}}{p_T^2}-2\right]\left[\frac{x^2}{z^2}+\left[1-\frac{x}{z}\right]^2\right]\right.$$
$$\left.+16(1-y)\frac{x^2}{z^2}\left[1-\frac{x}{z}\right]\right\}, \tag{2.4}$$

where $Q^2=xys$ and $\hat{s}=Q^2(z/x-1)$.

In Fig. 2 we show the ratio of the WWA prediction for $d\sigma(q\bar{q})/dp_T$ and the "exact" prediction according to Eq. (2.4) for various choices of $f_{\gamma|e}$. The short-dashed, dotted, and solid curves have been computed using the form (2.3) with different choices of $\bar{E}^2$, whereas the long-dashed curve has been obtained from the $f_{\gamma|e}$ function of Brodsky, Kinoshita, and Terazawa[19] which also contains terms that do not increase logarithmically with the electron energy. As we will see later, the region $p_T \lesssim 25$ GeV is of particular interest for the purpose of extracting $\mathbf{q}^\gamma$. Therefore, from now on we will choose $\bar{E}^2=x_p\bar{s}$, which is the squared energy of the photon-parton system, unless stated otherwise. This ansatz has also been shown[20] to reproduce the total $c\bar{c}$ and $b\bar{b}$ production cross sections quite well. However, for larger values of p_T the ansatz of Ref. 19 or even the simple choice[21] $\bar{E}=p_T$ work better.

Obviously, the two-jet cross section alone cannot be used to measure $\mathbf{q}^\gamma$, since it also depends on the parton densities inside the proton. This is demonstrated in Fig. 3 where we show the ratio R_σ of resolved-to-direct contributions to two-jet production as a function of p_T. Since we want to use the parametrization of $\mathbf{q}^\gamma$ as given in Ref. 22 as one of our standard choices, we have to choose $\Lambda_{\rm QCD}=0.4$ GeV. Here and in most of the remaining plots we have used $Q^2=p_T^2$, which is known[23] to reproduce S$p\bar{p}$S two-jet data quite well. In this case going from set 2 of Ref. 24 (DO2, solid curve) to the parametrizations of Ref. 25 (GHR, dotted curve) increases R_σ by only about 10% at small p_T and even less at larger p_T. This is, however, somewhat accidental; had we chosen[15] $Q^2=\hat{s}$ the two corresponding curves would differ by as much as 35% at small p_T. The reason for this strong dependence of even the ratio R_σ on $\mathbf{q}^p$ is that direct and resolved contributions probe quite different regions of x_p, especially for small values of p_T. Since the parton distributions inside the proton decrease rapidly with increasing x_p whereas the photon spectrum (2.3) is comparatively hard, the direct contributions are sensitive to $\mathbf{q}^p$ all the way down to $x_{\rm min}=4p_T^2/s$; on the other hand, the partons inside the photon obviously have less energy than the photon itself, which means that the resolved contributions probe larger values of x_p. Since the GHR parametrizations are valid only for $x_p \geq 0.01$ their prediction for the direct contributions are trustworthy only for $p_T \gtrsim 10$–15 GeV. For this reason we will from now on adopt the DO2 parametrizations for $\mathbf{q}^p$ as our standard choice. In the analysis of real HERA data they should be

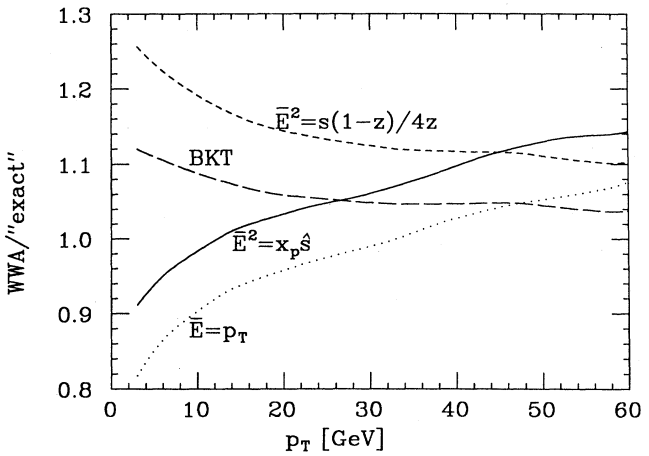

FIG. 2. The ratio of the cross section for the production of massless $q\bar{q}$ pairs as predicted by Weizäcker-Williams approximation, divided by the result of the "exact" calculation according to Eq. (2.4). Only the direct contribution from γg fusion is included. We have chosen the DO2 parametrization (Ref. 23) for $\mathbf{q}^p$, $Q^2=\hat{s}$, and $N_f=3$ for $Q^2\leq 50$ GeV^2; $N_f=4$ for 50 GeV$^2<Q^2\leq 500$ GeV^2; and $N_f=5$ for $Q^2>500$ GeV^2. For the dotted, solid, and short-dashed curves we have used the form (2.3) for $f_{\gamma|e}$ with different expressions for $\bar{E}$ as indicated, while for the long-dashed curve we have used $f_{\gamma|e}$ as given by Brodsky, Kinoshita, and Terazawa (Ref. 19).

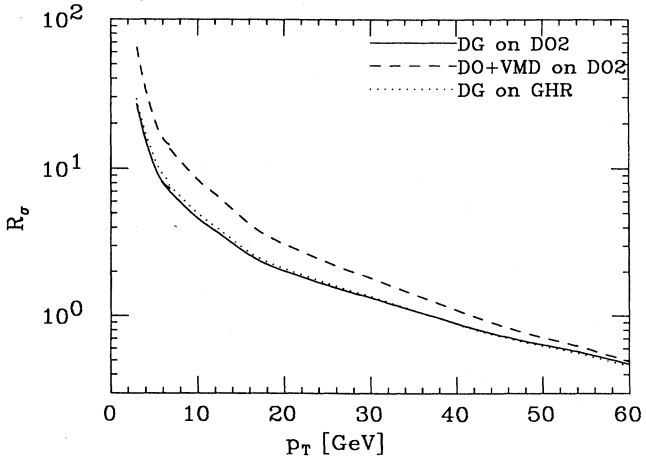

FIG. 3. The ratio R_σ of resolved to direct contributions to two-jet production at HERA. We have used $Q^2=p_T^2$, $N_f=4$, and $\bar{E}^2=\bar{s}x_p$. The three curves correspond to three different combinations of parametrizations for the parton densities inside the photon and proton, as indicated.

replaced by parton densities measured at the same machine. If one wants to analyze two-jet data down to $p_T = 5$ GeV, $\mathbf{q}^p$ has to be measured down to $x_p = 10^{-3}$. The quark distributions inside the proton at $x_p \gtrsim 10^{-3}$ can quite easily be measured at HERA via deep-inelastic scattering; for not too high values of Q^2, $G^p(x_p \gtrsim 10^{-3})$ can be measured[26] either via the longitudinal structure function or via the photoproduction of heavy flavors [see Sec. IV (Ref. 27)].

The dashed curve in Fig. 3 is for our second standard choice of parametrizations of $\mathbf{q}^\gamma$, which is a sum of the "asymptotic" part as parametrized in Ref. 14 and a vector-meson-dominance– (VMD–) inspired part (set I of Ref. 28). This assumption is necessary for our choice $\Lambda_{\rm QCD} = 0.4$ GeV since in this case the "asymptotic" part alone cannot describe data on F_2^γ. It should be stressed, however, that this ansatz is purely phenomenological;[14,21] in particular, the VMD part is taken to be independent of Q^2 which certainly overestimates its importance at large values of p_T. Furthermore, since the VMD-inspired contribution for F_2^γ is well behaved, this ansatz does nothing to cure the $x_\gamma \to 0$ divergences of the "asymptotic" prediction. Nevertheless, Fig. 3 tells us that a quantitative measurement of $\mathbf{q}^\gamma$ becomes more difficult with increasing p_T, since there the direct contributions become more important[12] and the differences in the predictions using different parametrizations of $\mathbf{q}^\gamma$ are less pronounced.

The reason for this last effect is that G^γ is much softer than q_i^γ; therefore, the contributions $\sim q_i^\gamma$ become more and more important with increasing p_T. This is demonstrated in Fig. 4(a) where we show the contributions of several different final states in the resolved case, where we have used the DG parametrization for $\mathbf{q}^\gamma$. Note that the qg final state receives contributions both from q_i^γ and from G^γ; however, for $p_T \geq 10$ GeV less than 25% of these events have a gluon out of the photon in the initial state. (Of course, this fraction can be larger for different choices for $\mathbf{q}^\gamma$.) Furthermore, since both parametrizations of $\mathbf{q}^\gamma$ agree with existing data on F_2^γ their quark distribution functions are quite similar, whereas the differences in G^γ are quite dramatic unless Q^2 becomes very large.

For comparison we show a similar plot for the direct contributions in Fig. 4(b). We see that because of the large gluon density in the proton, for $p_T \lesssim 30$ GeV it is dominated by photon-gluon fusion, leading to a $q\bar{q}$ final state. Note that the corresponding subprocess cross section[13] (just like that for $\gamma q \to gq$) only diverges like $\hat{t}^{-1}$ as $\hat{t} \to 0$ and would thus be set to zero in the approximation of Ref. 29, where only those processes are taken into account whose cross sections diverge as $\hat{t}^{-2}$ as $\hat{t} \to 0$, and which have facilitated[23] the determination of $\frac{4}{9}G(x) + \sum q(x)$ from two-jet data taken at the SPS $\bar{p}p$ collider. We find that this approximation works reasonably well for the resolved contributions, which it underestimates by 10–15 %. However, for reasons of consistency, and also because (unlike in the case of $p\bar{p}$ collisions) this approximation would not help too much to extract $\mathbf{q}^\gamma$ in our case (see Sec. III), we keep the full subprocess cross section everywhere.

From Figs. 3 and 4 we can draw the conclusion[15] that it will be fairly easy to use two-jet production at HERA to measure the quark content of the photon up to $Q^2 \simeq 2000$ GeV^2. However, the planned HERA detectors[30] will probably not be able to identify jets with p_T substantially below 10 GeV. It is therefore necessary to use more differential cross sections if we want to measure the gluon content of the photon via two-jet production. This is the topic of the next section.

III. THE RAPIDITY DISTRIBUTION OF HIGH-p_T JETS

The rapidity distributions of high-p_T jets have been successfully used[23,29] to determine parton densities inside the proton in $p\bar{p}$-collider experiments. In the present case

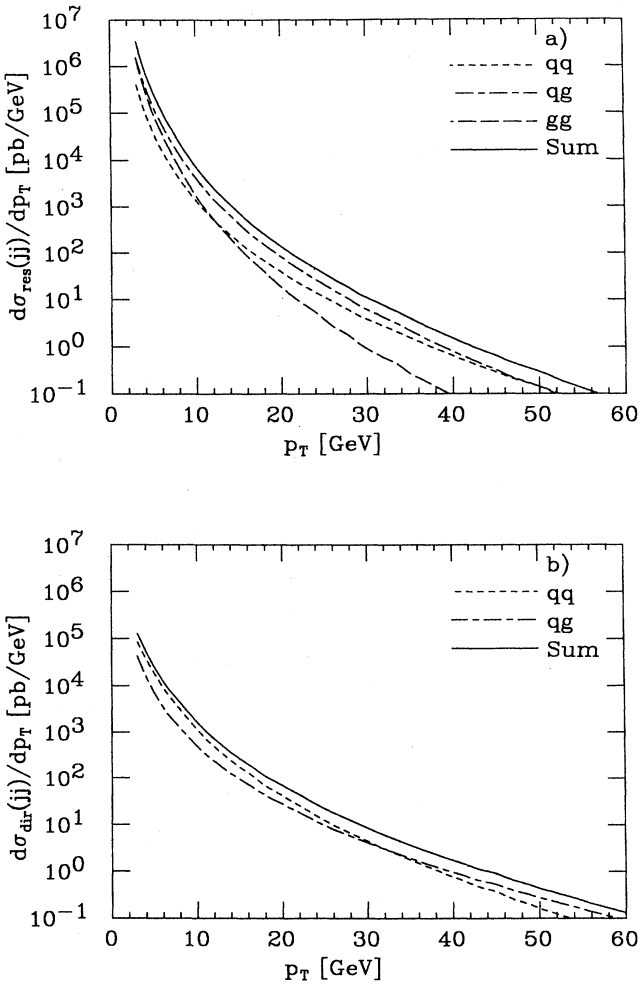

FIG. 4. Resolved (a) and direct (b) contributions to two-jet production, where the different final states are shown separately. Note that q denotes either a quark or antiquark. We have used the DO2 and DG parametrizations (Ref. 22) for $\mathbf{q}^p$ and $\mathbf{q}^\gamma$, respectively. The other parameters are as in Fig. 3.

this distribution is given by

$$\frac{d\sigma}{dp_T dy_1 dy_2} = V_p(x_p,Q^2)x_p z_{\min} \times \int_{z_{\min}}^1 \frac{dz}{z} f_{\gamma|e}(\bar{E},z) V_\gamma \left[\frac{z_{\min}}{z},Q^2\right] \times \frac{d\hat{\sigma}}{d\hat{t}}(\hat{s},\hat{t},\hat{u}) , \quad (3.1)$$

where

$$x_p = \tfrac{1}{2}x_T \left[\frac{E_e}{E_p}\right]^{1/2} (e^{y_1}+e^{y_2}) , \quad (3.2)$$

$$z_{\min} = \tfrac{1}{2}x_T \left[\frac{E_p}{E_e}\right]^{1/2} (e^{-y_1}+e^{-y_2}) \quad (3.3)$$

with

$$x_T^2 = \frac{4(m^2+p_T^2)}{s} , \quad (3.4)$$

where we have again allowed for nonzero (identical) final-state parton masses m. The jet rapidities y_1 and y_2 are measured in the laboratory frame, with $y>0$ corresponding to the direction of the proton beam, and $E_e=30$ GeV and $E_p=820$ GeV are the energies of the incoming electrons and protons in this frame. The other quantities in Eq. (3.1) are the same as in Eq. (2.1). Note that the cross section (3.1) has to be multiplied with $\frac{1}{2}$ if $y_1=y_2$, since in this case $\hat{t}=\hat{u}$ so that the two final-state jets have to be treated[28] as identical particles.

In this section we mainly focus on the *shape* of the rapidity distributions. We therefore normalize our curves for different choices of parameters such that $d\sigma(jj)/dp_T|_{p_T=10\text{ GeV}}=8830$ pb/GeV, which results if one chooses $Q^2=p_T^2$, $N_f=4$ flavors, $\bar{E}^2=x_p\bar{s}$, DO2 for $\mathbf{q}^p$ and DG (Ref. 15) for $\mathbf{q}^\gamma$, where both direct and resolved contributions have been included.

In Fig. 5 we show the remaining sensitivity to various choices of parameters except $\mathbf{q}^\gamma$, for which we have used the DG parametrization. The solid curve has been obtained with parameters as listed above. For the long-dashed curve we have used the same parameters except that we have used the Brodsky-Kinoshita-Terazawa[19] form for $f_{\gamma|e}$, multiplied with 0.97; obviously the differences are negligibly small. The difference between the solid and short-dashed curves is that the latter has been obtained using the GHR parametrization for $\mathbf{q}^p$, multiplied with 1.01. Since these are somewhat harder than DO2, it prefers larger rapidities. (Recall that positive y means the proton direction.) The dotted curve finally is again for DO2 parametrizations, but with $Q^2=\hat{s}$, multiplied with 1.4. Note that $y_1=y_2$ leads to the smallest possible values of $\hat{s}$, $\hat{s}=4p_T^2$; normalizing the total contribution at $p_T=10$ GeV gives a bigger cross section at $y_1=y_2$ for $Q^2=\hat{s}$ than for $Q^2=p_T^2$ since $\sigma\sim\alpha_s\sim 1/\ln Q^2$. The comparison between the dotted and solid curves also shows that $\mathbf{q}^p(Q^2=4p_T^2)$ is already quite a bit softer than $\mathbf{q}^p(Q^2=p_T^2)$ so that the rapidity distribution has its maximum at smaller values of y.

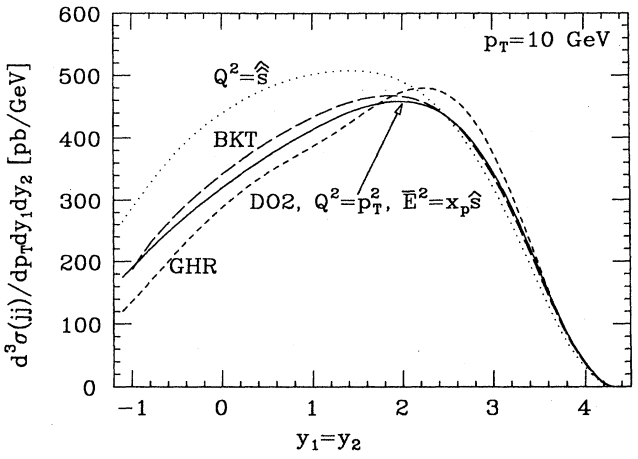

FIG. 5. Triple-differential two-jet cross section at HERA for $p_T=10$ GeV as a function of $y_1=y_2$, where we have used the DG parametrization for $\mathbf{q}^\gamma$ and $N_f=4$. The remaining parameters for the solid curve are chosen as in Fig. 4, whereas the dotted curve is valid for $Q^2=\hat{s}$. For the short-dashed curve we have chosen the GHR parametrization (Ref. 25) for $\mathbf{q}^p$, while for the long-dashed curve we have used the BKT form (Ref. 19) for $f_{\gamma|e}$. The dotted, short-dashed, and long-dashed curves have been multiplied with 1.4, 1.01, and 0.97, as described in the text.

One common property of all curves of Fig. 5 is that they approach zero as $y\to y_{\max}=\ln[(1/x_T)(E_p/E_e)^{1/2}]$ whereas they remain finite as $y\to y_{\min}=-\ln[(1/x_T)(E_e/E_p)^{1/2}]$. The first case corresponds to $x_p\to 1$, which obviously implies $\mathbf{q}^p\to 0$. In the second case one has $z_{\min}=z\cdot x_\gamma\to 1$; this implies $\mathbf{q}^\gamma\to 0$, but since $f_{\gamma|e}$ remains finite in this limit, the direct process still contributes. From Figs. 6(a) and 6(b) we see that the direct contribution is in fact maximal for $y=y_{\min}$, which corresponds to $x_p=x_{p,\min}=x_T^2$, due to the sharp spike of the gluon and sea-quark distributions inside the proton at small x_p.

These figures also show that the rapidity distribution of the jets might help to disentangle the various resolved contributions, and especially to measure G^γ. The quark distributions inside the photon have a very hard component, which peaks around $x_\gamma=0.9$ and consequently allows x_p to be rather small [recall that in the given case $y_1=y_2$, Eqs. (3.2)–(3.4) give $x_p x_\gamma z=x_T^2$]; processes that are initiated by a quark from the photon therefore make sizable contributions already at small and even negative rapidities. Since the q_i^γ also have a spike at $x_\gamma\to 0$, the overall rapidity spectrum of these processes is rather flat. This is demonstrated by the curves for two quarks (short-dashed curve) and one quark and one gluon (long-short-dashed curve); already at $p_T=10$ GeV, Fig. 6(a), the overall resolved contribution to these final states comes to 95% (qq) and 75% (qg) from events which have a quark from the photon in the initial state. On the other hand, G^γ is a steadily falling function of x_γ. The contribution from the two-gluon final state (long-dashed curves), more than 95% of which are also initiated by

two gluons, has therefore a pronounced maximum at large rapidities.

Not surprisingly, the comparison between Figs. 6(a) and 6(b) shows that processes which are initiated by partons with a soft spectrum die out faster as p_T increases; the contributions proportional to G^γ are quite a bit smaller than those proportional to q_i^γ for all rapidities, and the direct contributions become much more important (also see Fig. 2), even at large rapidities. Under these circumstances, a direct measurement of G^γ would obviously be next to impossible.

In Fig. 7(a) we therefore compare the shape of the rapidity distribution at $p_T=10$ GeV for several choices of $\mathbf{q}^\gamma$. The solid curve is for the DG parametrization and the dashed curve for the sum of "asymptotic" and VMD parametrizations, multiplied with 0.62 to give the same $d\sigma(jj)/dp_T$ at $p_T=10$ GeV; for the dotted curve we have again used the DG parametrization, but with $G^\gamma=0$ and multiplied with 1.5. Obviously, the presence of gluons inside the photon has quite a dramatic effect on the shape of the rapidity distribution, shifting its maximum towards larger rapidities. Since the sum DO+VMD has a much larger G^γ than DG, the corresponding curve shows a much more pronounced maximum, even though the position of the maximum is more or less the same.

For comparison we show the corresponding results for $p_T=20$ GeV in Fig. 7(b), where the dotted, solid, and lower dashed curves have been obtained with the *same* normalization factors as at $p_T=10$ GeV. In fact, the differences between these three curves is now mostly due to these factors; the differences in the shape of the curves are smaller than in Fig. 7(a). This is demonstrated by the upper-dashed curve which has been normalized to give the same $d\sigma(ij)/dp_T$ at $p_T=20$ GeV as the DG parametrization for $\mathbf{q}^\gamma$. We note again that our use of a Q^2-independent VMD-type part in $\mathbf{q}^\gamma$ overestimates the importance of this contribution especially at high values of Q^2, i.e., large p_T.

We conclude from Fig. 7 that a measurement of the jet rapidity distribution should not only reveal the presence of a nonzero G^γ but also allow for an at least semiquantitative measurement of this gluon distribution function inside the photon. However, for a more precise determina-

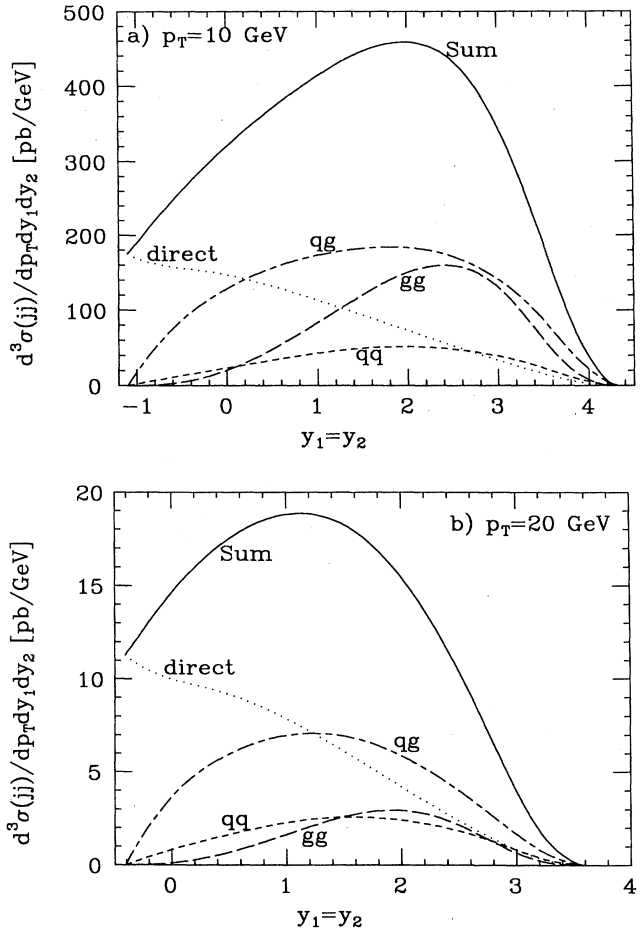

FIG. 6. Triple-differential two-jet cross section at HERA as a function of $y_1=y_2$ for (a) $p_T=10$ GeV and (b) $p_T=20$ GeV. The dotted curves show the direct contribution. The meaning of the dashed curves, as well as the choice of parameters, is as in Fig. 4(a).

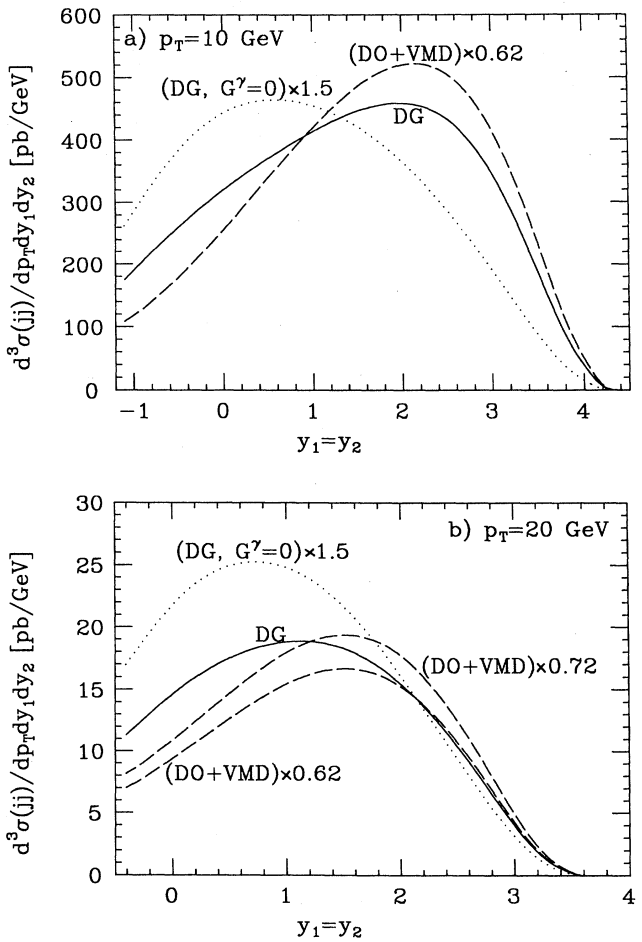

FIG. 7. Comparison of the shape of the jet rapidity distributions for (a) $p_T=10$ GeV and (b) $p_T=20$ GeV. Note that the dotted and dashed curves have been normalized, as discussed in the text. The remaining parameters are as in Fig. 4.

tion one would have to get rid of those resolved contributions which are initiated by quarks from the photon, since they dominate the resolved contributions for $p_T \gtrsim 10$ GeV. One possibility to achieve this goal is to look at the production of heavy $q\bar{q}$ pairs with $q=c$ or b.

IV. BOTTOM PRODUCTION AT HERA

In Ref. 15 we have shown that the contribution to total charm and bottom production that comes from gluon-gluon fusion is at least 3 to 4 times larger than the quark-antiquark annihilation contribution, while the direct-photon–gluon-fusion process is bigger by another factor of 2–4, depending on the parametrizations used (see also Ref. 31). This shows that if we are able to somehow separate direct from resolved contributions, heavy-quark production will offer a good possibility to measure G^γ directly. In this paper we focus on $b\bar{b}$ production since it seems to be significantly easier to tag on b quarks than on c quarks. Another advantage of b quarks is that the smaller electric charge leads to a relative suppression of the direct contribution. Finally, since the b quark is substantially heavier than the c quark its fragmentation function is expected[32] to be harder, which means that the differences between distributions for b quarks, which we will show, and the corresponding distributions for b quark containing hadrons, which will be measured, are rather small.

In Sec. III we have seen that at least for massless final-state partons rapidity distributions offer a powerful tool to achieve this separation. In Fig. 8 we show $d^3\sigma(b\bar{b})/dp_T dy_1 dy_2$ as a function of y_2 for three different values of y_1, where we have used the DO2 parametrization for $\mathbf{q}^p$, DO+VMD for $\mathbf{q}^\gamma$, $Q^2=p_T^2+m_b^2$ with $m_b=5$ GeV, and $N_f=4$ flavors; the relevant QCD subprocess cross sections have been taken from Ref. 33. The dotted curves show the contribution of direct photon-gluon fusion, whereas the solid curves represent the sum of direct and resolved contributions.

We first note that choosing *one* rapidity to be negative, $y_1=-1$, effectively removes all resolved contributions even for the big G^γ chosen for this figure. Note that this restriction still allows us to probe $G^p(x_p)$ for x_p between 2×10^{-3} and 1 by varying y_2 within its kinematically allowed limits [see Eqs. (3.2)–(3.4)]. This should allow for a quite accurate measurement of the gluon distribution inside the proton at all necessary values of x_p, which has to be done before G^γ can be measured. On the other hand, if we want to significantly suppress the direct contributions we require both the b and the $\bar{b}$ quark to have rather large, positive rapidities. From now on we will therefore choose $y_1=y_2$.

From Fig. 9 we see that a good measurement of G^γ will only be possible if b quarks with a transverse momentum of less than 10 GeV can be reliably identified; otherwise the cross section at the high rapidities necessary to suppress the direct contributions will be too small to allow for the accumulation of a sufficiently large number of events. (Note that the design luminosity at HERA is 1.6×10^{31} cm^{-2}sec^{-1}, which corresponds to roughly 100 events per year of running time for a cross section of 1 pb.) It would be ideal if b quarks with a transverse momentum as small as 3 GeV could be detected, since here both the cross section and the ratio of resolved-to-direct contributions have their maximum.

In Fig. 10 we show the rapidity distribution of the b (or $\bar{b}$) quarks at $p_T=5$ GeV; direct, gg, and $q\bar{q}$ contributions are shown separately, and we have used the DG parametrization for $\mathbf{q}^\gamma$. Obviously, the direct contribution is a serious background to the contribution from gg fusion even at the largest accessible rapidities, at least for this parametrization of the parton densities inside the photon.

In Fig. 11 we therefore again resort to comparing the shape of the rapidity distribution for different parametrizations of $\mathbf{q}^\gamma$. As expected, more gluon inside the pho-

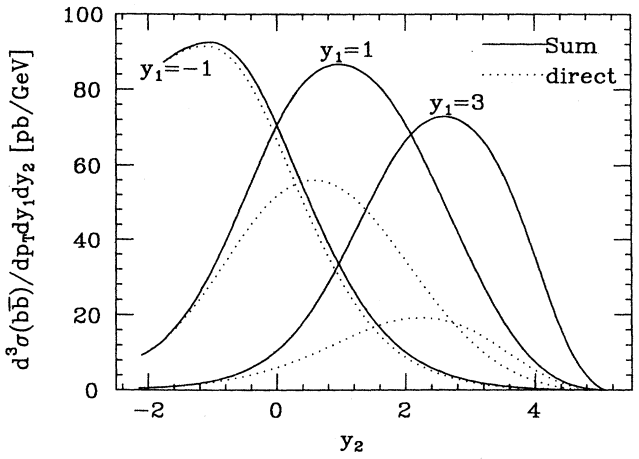

FIG. 8. Rapidity distributions of the b (or $\bar{b}$) quark at $p_T=5$ GeV. The dotted curves show only the direct contribution to $b\bar{b}$ production, whereas the solid curves show the sum of direct and resolved contributions. We have used the DO+VMD and DO2 parametrizations for $\mathbf{q}^\gamma$ and $\mathbf{q}^p$, respectively, $Q^2=p_T^2+m_b^2$, $m_b=5$ GeV, $N_f=4$, and $\bar{E}=\bar{s}x_p$.

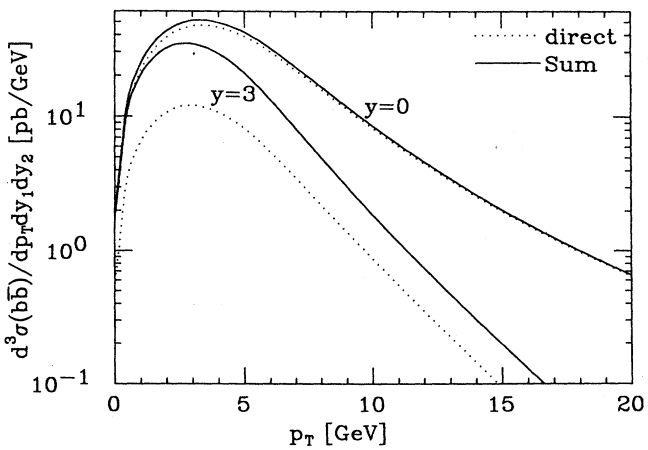

FIG. 9. Transverse-momentum distribution of the b (or $\bar{b}$) quark for $y_1=y_2\equiv y$, where we have used the DG parametrization for $\mathbf{q}^\gamma$. Notation and the other parameters are as in Fig. 8.

ton leads to a flatter distribution. As in the case of two-jet production we conclude that the presence of gluons inside the photon should be detectable, but that a good measurement of G^γ will probably only be possible if the background from direct photon-gluon fusion can be eliminated.

V. THE SPECTATOR JET FROM THE PHOTON

One possibility to separate the direct from the resolved contributions is to tag on the spectator jet from the photon, which is only produced if the photon is split into quarks and gluons, i.e., in the resolved case (see Fig. 1). Unfortunately, this jet goes into the direction of the electron beam and might therefore be missed by the planned HERA detectors[30] which focus on particles flying in the direction of the proton. However, our previous discussion shows that it might be worthwhile to incorporate the possibility to tag on the existence of this second spectator jet, even if one will not be able to measure its energy accurately.

The question of whether or not a given detector will see this jet depends crucially on how broad it is, i.e., on the average angle between particles in the jet and the beam pipe. Unfortunately, we do not know of any experimental information on the properties of spectator jets that originate from photons. We can therefore only give a crude estimate of the opening angle of the spectator jet.

In Fig. 12 we show the average energy of the spectator jet in the laboratory frame for two-jet events; the parameters are chosen as in Fig. 6(a). Since the bulk of the resolved contribution comes from positive rapidities we can conclude that the typical spectator jet energy is about 10 GeV, i.e., $\langle z(1-x_\gamma)\rangle \simeq \frac{1}{3}$. Assuming a multiplicity of $n=10$ particles in the jet and an average intrinsic transverse momentum of 300 MeV we estimate the opening angle θ,

$$\theta \simeq \frac{n\langle p_T\rangle}{\langle E_{\text{spec jet}}\rangle} \simeq 15^\circ , \tag{5.1}$$

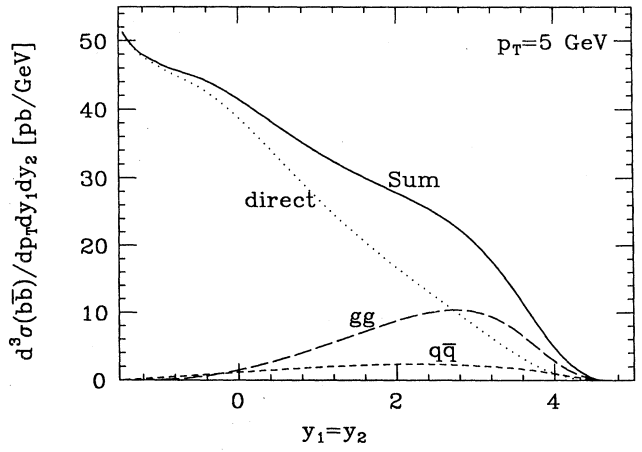

FIG. 10. Various contributions to the b- ($\bar{b}$-) quark rapidity distribution at $p_T=5$ GeV. Parameters are the same as in Fig. 9.

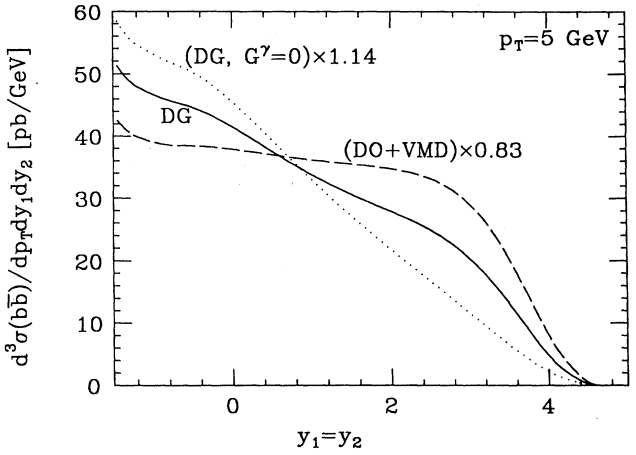

FIG. 11. Comparison of the shape of the b- ($\bar{b}$-) quark rapidity distribution at $p_T=5$ GeV for various parametrizations for q^γ; the dotted and dashed curves are normalized as discussed in the text. The remaining parameters are the same as in Fig. 8.

which should make the jet easily detectable. Note that the multiplicity, and thus θ, might very well be higher, since presumably the properties of the spectator jet are governed by its energy in the γp center-of-mass system, which is the natural reference frame in our problem. In this frame one finds $\langle E_{\text{spec jet}}\rangle \simeq 70$ GeV, which might imply a rather large multiplicity.

If our estimate (5.1) is realistic, one might even hope to measure the energy of the spectator jet. From Fig. 12 we see that this would help to separate events that have a gluon from the photon in the initial state, since these events tend to have a harder spectator jet; the reason is, of course, that the gluon distribution inside the photon is much softer than the quark distribution. Note, however,

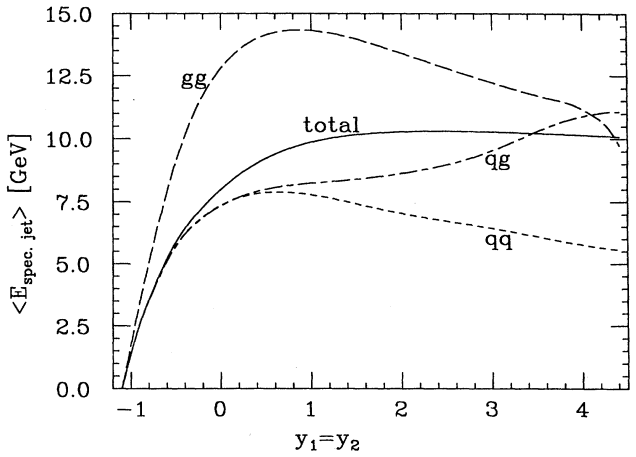

FIG. 12. The average energy (in the laboratory frame) of the photon spectator jet for HERA events with two high-p_T jets for $p_T=10$ GeV. Predictions for events with different final states are shown separately. Note that only resolved contributions are included in the average. Parameters are the same as in Fig. 4.

that a substantial part of the spectator jet energy might be carried away by one or two leading particles, which would most probably vanish in the beam pipe; in this case even the difference of a factor 2 between the average spectator jet energies of gg-initiated versus qq-initiated events might be hard to measure. Note that the difference between the qq and the qg results at large rapidities is entirely due to the contribution to the qg final state that has a gluon from the photon in the initial state; even though this $G^{\gamma}q^{p}$ combination only contributes about 25% of the total resolved qg final-state cross section at $p_T=10$ GeV, it dominates at large rapidities, which again reflects the large difference in the shape of the quark and gluon distributions inside the photon.

In Fig. 12 we have chosen $p_T=10$ GeV, but the three dashed curves would look very similar at different values of p_T. Since the relative importance of events with a quark from the photon in the initial state increases with p_T, see Fig. 4(a), the total average spectator jet energy falls with increasing p_T.

In the last section we have seen that the resolved contribution to $b\bar{b}$ production is dominated for gg fusion. From Fig. 12 we therefore expect the average spectator jet energy for $b\bar{b}$ production to be larger than for two-jet production. This is demonstrated in Fig. 13 where we show the average spectator jet energy for both the DG parametrization (solid) and for the DO+VMD parametrization (dashed). The difference between these two curves at very large rapidities is very interesting, since it is a direct consequence of the sharp $x_{\gamma}\to 0$ spike of the "asymptotic" part of $\mathbf{q}^{\gamma}$. Unfortunately, the cross section at these large rapidities is already rather small; see Fig. 10.

VI. SUMMARY AND CONCLUSIONS

In this paper we have studied the question whether the forthcoming ep collider HERA can be used to measure the hadronic structure and, especially, the gluon content of the photon. This measurement is of some importance since it might settle the ongoing[8] debate about how to compute $\mathbf{q}^{\gamma}(x_{\gamma},Q^2)$ within the framework of perturbative QCD.

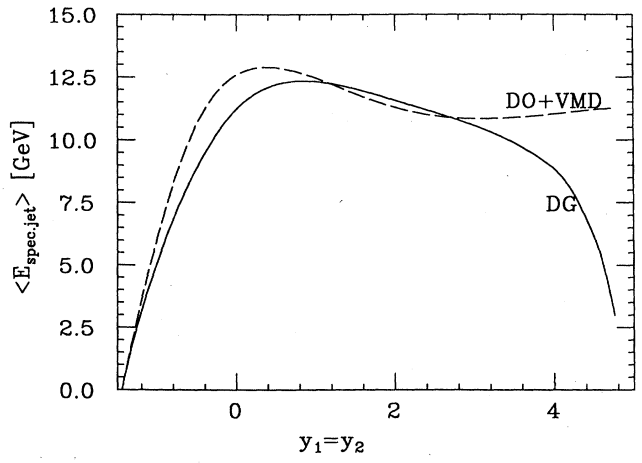

FIG. 13. The average energy of the photon spectator jet for the resolved contribution to $b\bar{b}$ production for $p_T=5$ GeV and two different parametrizations of $\mathbf{q}^{\gamma}$. The remaining parameters are as in Fig. 8.

An obvious condition for the determination of the parton densities inside the photon at HERA is a good knowledge of the parton densities inside the proton, since all relevant cross sections are proportional to the product of these two quantities. Fortunately, the proton structure can be measured independently at HERA. It should be rather easy to measure the quark distribution functions at all relevant x_p via deep-inelastic scattering; G^{p} can, e.g., be measured via $b\bar{b}$ production if one requires the rapidity of one of the heavy quarks to be negative, which eliminates almost all events where the photon is resolved into quarks and gluons, as we have shown in Sec. IV (see Fig. 8).

The answer to the question how well $\mathbf{q}^{\gamma}$, and especially G^{γ}, can be measured at HERA once $\mathbf{q}^{p}$ is known depends crucially on how well the spectator jet from the photon, which characterizes the resolved contributions (see Fig. 1), can be measured.

In the most optimistic case this jet cannot only be detected, but it is also possible to get a good idea of its energy. In this case the spectator jet cannot only be used to discriminate between direct and resolved contributions, but also to distinguish events that have a quark from the photon in the initial state from those initiated by a gluon from the photon, since in the latter case the spectator jet is on the average twice as energetic, see Fig. 12. In this case G^{γ} can be "directly" measured not only in $b\bar{b}$ production, but also in ordinary two-jet production, which allows for a direct consistency check of the whole approach.

If the presence of the second spectator jet can be detected, but its energy cannot be measured, a fairly direct determination of G^{γ} from $b\bar{b}$ production should still be possible. A prerequisite for this is, of course, a bottom trigger that is both reliable in discarding events without b quarks and not too inefficient in detecting events with b quarks; recall that the resolved contribution to $b\bar{b}$ production is only a few pb per GeV and rapidity unit, see Fig. 10. Using G^{γ} as measured by this method and the q_i^{γ} as measured in $e^{+}e^{-}$ collisions one can predict the two-jet rate; a comparison with the measured rate provides a consistency check even in this less favorable case.

We feel that the second spectator jet should be detectable unless our estimate (5.1) of its opening angle is completely wrong. Since experimentally nothing is known about the properties of this jet, this possibility can at present not be excluded. Even in this case the presence of a sizable gluon content inside the photon should lead to visible effects in the shape of the rapidity distribution of jets (Fig. 7) and b quarks (Fig. 11); here we assume that hadronization and fragmentation effects do not grossly change these distributions. This assumption seems to be justified by the successful measurement of parton densities in $p\bar{p}$ collisions.[22] However, in this least favorable case a quantitative determination of G^{γ} will only be pos-

sible by means of an overall fit to the data.

In summary, we think that HERA experiments have a good chance to measure the gluon content of the photon and thus to settle the ongoing dispute on how to compute the photon structure function, if the spectator jet from the photon can be seen. Since this measurement is of interest not only for particle physicists but might also allow us to understand the structure of air showers that are initiated by very energetic photons[34] we feel that trying to see this spectator jet is well worth the effort.

ACKNOWLEDGMENTS

We are indebted to B. Diekmann, X. Tata, K. Hikasa, S. Willenbrock, and D. Morris for discussions. The work of R.M.G. was supported by the Bundesministerium für Forschung und Technologie, Bonn. The work of M.D. was supported in part by the University of Wisconsin Research Committee with funds granted by the Wisconsin Alumini Research Foundation, and in part by the U.S. Department of Energy under Contract No. DE-AC02-76ER00881.

---

*On leave of absence from University of Bombay, India.

[1]E. Witten, Nucl. Phys. **B120**, 189 (1977).

[2]W. A. Bardeen and A. J. Buras, Phys. Rev. D **20**, 166 (1979); **21**, 2041(E) (1980).

[3]R. J. DeWitt *et al.*, Phys. Rev. D **19**, 2046 (1979).

[4]D. W. Duke and J. F. Owens, Phys. Rev. D **22**, 2280 (1980); G. Rossi, Phys. Lett. **130B**, 105 (1983); Phys. Rev. D **29**, 852 (1984).

[5]M. Glück and E. Reya, Phys. Rev. D **28**, 2749 (1983).

[6]I. Antoniadis and G. Grunberg, Nucl. Phys. **B213**, 445 (1983).

[7]M. Glück, K. Grassie, and E. Reya, Phys. Rev. D **30**, 1447 (1984).

[8]For a defense of the regularization procedure suggested in Ref. 6, see I. Antoniadis and L. Marleau, Phys. Lett. **161B**, 163 (1985); for a critique, see J. H. Field, F. Kapusta, and L. Poggioli, Phys. Lett. B **181**, 362 (1986); Z. Phys. C **36**, 121 (1987). The question of the input distributions $\mathbf{q}^{\gamma}(Q_0^2)$ is also discussed in J. H. Da Luz Vieira and J. K. Storrow, University of Manchester Report No. THM/C8728, 1987 (unpublished); M. Glück and E. Reya, University of Dortmund Report No. DO-TH 88/7, 1988 (unpublished).

[9]For a recent review, see J. Olsson, in *Lepton and Photon Interactions,* proceedings of the International Symposium on Lepton and Photon Interactions at High Energies, Hamburg, West Germany, 1987, edited by R. Rückl and W. Bartel [Nucl. Phys. B, Proc. Suppl. **3** (1987)].

[10]W. Wagner, in *Proceedings of the 23rd International Conference on High Energy Physics,* Berkeley, California, 1986, edited by S. C. Loken (World Scientific, Singapore, 1987).

[11]M. Drees, M. Glück, K. Grassie, and E. Reya, Z. Phys. C **27**, 587 (1985).

[12]J. Owens, Phys. Rev. D **21**, 54 (1979).

[13]D. W. Duke and J. Owens, Phys. Rev. D **26**, 1600 (1982).

[14]P. Aurenche, R. Baier, A. Douiri, M. Fontannaz, and D. Schiff, Nucl. Phys. **B286**, 553 (1987).

[15]M. Drees and R. M. Godbole, Phys. Rev. Lett. **61**, 682 (1988).

[16]C. F. Weizsäcker, Z. Phys. **88**, 612 (1934); E. J. Williams, Phys. Rev. **45**, 729 (1934).

[17]B. L. Combridge, J. Kripfganz, and J. Ranft, Phys. Lett. **70B**, 243 (1977); M. Glück, J. Owens, and E. Reya, Phys. Rev. D **18**, 1501 (1978).

[18]G. A. Shuler, DESY Report No. 87-114, 1987 (unpublished).

[19]S. J. Brodsky, T. Kinoshita, and H. Terazawa, Phys. Rev. D **4**, 1532 (1971); see also H. Terazawa, Rev. Mod. Phys. **45**, 615 (1973).

[20]M. Glück, R. M. Godbole, and E. Reya, Z. Phys. C (to be published).

[21]P. Aurenche, R. Baier, M. Fontannaz, and D. Schiff, University of Paris report, 1988 (unpublished).

[22]M. Drees and K. Grassie, Z. Phys. C **28**, 451 (1985).

[23]For a review, see J. R. Cudell, F. Halzen, and C. S. Kim, Int. J. Mod. Phys. **A3**, 1051 (1988).

[24]D. W. Duke and J. Owens, Phys. Rev. D **30**, 49 (1984).

[25]M. Glück, E. Hoffman, and E. Reya, Z. Phys. C **13**, 119 (1982).

[26]A. D. Martin, R. G. Roberts, and W. J. Stirling, Phys. Rev. D **37**, 1161 (1988).

[27]The difference between "conventional" gluon distributions which evolve from an input $x\cdot G^p(x,Q_0^2)\to$const as $x\to 0$ (e.g., Refs. 24 and 25) on the one hand, and the much steeper ansatz $xG^p(x,Q_0^2)\to 1/\sqrt{x}$ (set III of Ref. 26) suggested by the resummation of subleading logarithms, or the even steeper gluon distribution predicted by the dynamical generation of sea-quark and gluon distributions [see M. Glück, R. M. Godbole, and E. Reya, University of Dortmund Report No. DO-TH 88-9, 1988 (unpublished)] on the other hand, becomes quite sizable for $x_p \lesssim 10^{-3}$. Hence, it might be safer not to use the two-jet distribution below $p_T=5$ GeV in our study.

[28]See Da Luz Vieira and Storrow (Ref. 8).

[29]B. L. Combridge and C. J. Maxwell, Nucl. Phys. **B239**, 429 (1984).

[30]For a review, see G. Wolf, in *New Frontiers in Particle Physics,* proceedings of the Lake Louise Winter Institute, Lake Louise, Canada, 1986, edited by J. M. Cameron, B. A. Campbell, A. N. Kamal, and F. C. Khanna (World Scientific, Singapore, 1986), p. 144.

[31]R. K. Ellis and Z. Kunszt, Report No. FERMILAB-Pub-87/226-T, 1987 (unpublished).

[32]For a review, see T. Sjöstrand, Int. J. Mod. Phys. **A3**, 751 (1988).

[33]B. L. Combridge, Nucl. Phys. **B151**, 429 (1979); see also M. Glück, J. Owens, and E. Reya, Phys. Rev. D **17**, 2324 (1978).

[34]M. Drees and F. Halzen, Phys. Rev. Lett. **61**, 275 (1988).